Biochemical and Biophysical Research Communications 530 (2020) 42–46

Contents lists available at ScienceDirect

Biochemical and Biophysical Research Communications

journal homepage: www.elsevier.com/locate/ybbrc

Crystal structure of ClA1, a type of chlorinase from soil bacteria

Ya Miao [a], Jin Yu [b], Zhuqing Ouyang [a], Huihua Sun [c, **], Yan Li [a, *]

[a] Department of Pathogen Biology, School of Basic Medicine, Tongji Medical College, Huazhong University of Science and Technology, 13 Hangkong Road, Wuhan, Hubei, 430030, China
[b] National Demonstration Center for Experimental Basic Medical Education (Huazhong University of Science and Technology), 13 Hangkong Road, Wuhan, Hubei, 430030, China
[c] Metabolic Engineering Research Laboratory (MERL), Singapore Institute of Food and Biotechnology Innovation, Agency for Science, Technology and Research, 31 Biopolis Way, Nanos #01-01, 138669, Singapore

ARTICLE INFO

Article history:
Received 22 June 2020
Accepted 24 June 2020
Available online 29 July 2020

Keywords:
ClA1
Chlorinase
Crystal structure

ABSTRACT

Halogenated compounds are widely discovered in nature, and many of them exhibit biological activities, such as an important chlorinated natural product salinosporamide A serving as a potential anticancer agent. Compared with bromination, iodination and fluorination, chlorination is the mainly important modification. To shed light on the mechanism of SAM-dependent chlorinases, a recombinant chlorinase ClA1 was expressed in *Escherichia coli* and further purified for crystallization and X-ray diffraction experiments. The flake crystals of ClA1 were able to diffract to a resolution of 1.85 Å. The crystals belonged to space group R3, with unit-cell parameters $\alpha = \beta = 90.0°$, $\gamma = 120.0°$. By determining the structure of ClA1, it is revealed that the side chain of Arg242 in ClA1 may have contacts with the L-Met. However, in SalL the equivalent Arg243's side chain is far from L-Met. Considering the ClA1 and SalL are from different environments and their enzyme kinetics are quite different, it is suggested that the side chain conformation differences of the conserved arginine are possibly related with the enzyme activity differences of the two chlorinases.

1. Introduction

S-Adenosylmethionine (SAM) is one of the most important enzyme substrate and can support enzymes with methyl groups to methylate many substrates [1]. Methylation is able to regulate gene expression and increases the activity of specialized metabolites in the development of anti-cancer drugs [2]. In coordinating pericyclic reaction, SAM serves as a cofactor by electrostatic catalysis [3]. Another important role of SAM is serving as a substrate which can be catalyzed by halogenases from 5′-halo-5′-deoxyadenosine (XDA), and this reaction use nucleophilic substitution mechanism [4–6]. In traditional way, the synthetic yield of SAM and SAM analogs are low and lack of diatereoselectivity [7], while chemoenzymatic synthesis is demonstrated as a more effective way [8]. SalL is a type of chlorinase discovered from the marine bacteria. SalL can catalyze SAM and chloride ions to 5′-chloro-5′-deoxyadenosine and L-methionine, and this reaction is reversible. The downstream application like methylation and alkylation by methyltransferases *in situ* could couple with chemoenzymatic synthesis of SAM or analogs [9]. Recently, Sun and co-workers identified two new SAM-dependent chlorinases, ClA1 and ClA2, through BLAST search. Interestingly, ClA1 and ClA2 are both from soil bacteria, unlike SalL from marine bacteria [10].

Halogen atom can amplify biological activity, and the different halogen atoms (fluorine, chlorine, bromine, and iodine) have different chemical properties, such as relative electronegativity, nucleophilicity. Moreover, the size of halides deeply influence halogenases to select particular halides [11]. The first halogenating enzyme was found in 1959. The enzyme was named as chloroperoxidase since it required hydrogen peroxide [12], and many chloro-, bromo-, and iodoperoxidase were following detected. The most commonly utilized halogen atoms in the natural product biosynthesis are the chloride or bromide. There are only about 120 known iodinated examples and 30 fluorinated natural products [13]. The scarcity of iodinated and fluorinated products not only reflect the low natural abundance of iodine but also prove the fluoride ion is an inert [14,15]. Halogenases catalyze various substrates with numerous ways such as oxidation, reduction, and substitution.

* Corresponding author.
** Corresponding author.
E-mail addresses: sun_hui_hua@sifbi.a-star.edu.sg (H. Sun), yanli@hust.edu.cn (Y. Li).

https://doi.org/10.1016/j.bbrc.2020.06.129
0006-291X/

However, halogenated molecules particularly the anthropogenic molecules are often regarded as pollutant because they are difficult to degrade and harmful to human beings and animals. According to this, degradation and bioremediation are necessary. Microbial dehalogenation acts as a key part for a biogeochemical halogen cycle. Indeed, biocatalysts are able to remove halogens from compounds [16,17]. Halogenating enzymes have three types, including H_2O_2-requiring haloperoxidases, the oxygen-dependent halogenases and the nucleophilic halogenases [18,19]. Halogen substituents can deeply influence the biological activity of many natural products. For example, when a chlorine atom of vancomycin is displaced by a hydrogen, the antibacterial activity will sharply decrease [20]. Besides, another example worth mentioning is the chlorinated anticancer candidate Salinosporamide A (SalA) which is the chlorinated marine natural product from *Salinispora tropica*. SalA is also served as a potent 20s proteasome inhibitor currently in phase 1 human clinical trials for the treatment of multiple myeloma [21–27]. Compared with its deschloro analog Salinosporamide B (SalB), SalA is 500 times more active. The most organohalogen natural products are chlorinated, because chloride is widely found in marine and terrestrial environments, indeed, chloride has higher content in seawater than soil. According to some studies, they have clarified the catalytic origin of the catalytic efficiency of SalL. It was shown that the active sites offer electrostatic stabilization of the transition state and the catalytic efficiency depends on the solvation of Cl^- by the protein rather than the desolvation [28].

Given the biological importance of the enzyme, it's essential to figure out catalytic power, in particular, the active site architecture and halide binding site through its structure. In this study, we report the expression, purification and structure determination of ClA1 which is possibly to help understand the enzyme activity.

2. Materials and methods

2.1. Cloning, expression and purification

The gene was amplified with forward and reverse primers containing Nde1 and Xho1 restriction sites (Supplementary Table 1). The ClA1 gene was ligated into a pET-28a expression vector to attach an N-terminal histidine tag and placed into an *Escherichia coli* BL21(DE3) cell line. *E.coli* cultures were grown at 37 °C in 400 mL 2 × YT medium supplemented with 30 mg/mL kanamycin until they reached an OD_{600} of between 0.6 and 0.8, and protein expression was induced by the addition of 0.5 mM isopropyl β-D-1-thiogalactopyranoside and the cell were allowed to grow 20 h at 16 °C. Then the bacteria were harvested by centrifugation at 7000*g* for 10 min at 16 °C and were resuspended in lysis buffer consisting of 20 mM Tris-HCl pH 7.5, 200 mM NaCl and 1 mM benzamidine. The cells were lysed by sonication on ice and the soluble supernatant was collected by centrifugation at 13000*g* for 30 min at 4 °C. The supernatant was passed through a gravity column with 2 mL Ni-NTA Agarose that had previously been equilibrated with lysis buffer. After washing the protein respectively with 15 mL 10 mM imidazole and 30 mM imidazole containing 20 mM Tris-HCl pH 7.5, 200 mM NaCl. Subsequently the ClA1 protein was eluted from the column with 10 mL elution buffer (20 mM Tris-HCl pH 7.5, 200 mM NaCl and 300 mM imidazole). The flow-through was concentrated to 2 mL in centrifugal concentrators (Millipore, 10 KDa cutoff), and loaded onto a Superdex 75 pg HiLoad 16/600 gel-filtration column (GE Healthcare) equilibrated with 30 mM Tris-HCl pH 8.0, 150 mM NaCl and 2 mM DTT. The purity of the fractions containing the protein was checked by SDS-PAGE analysis.

2.2. Crystallization and preliminary X-ray analysis

After size-exclusion chromatography, the purest peak fractions of ClA1 were pooled and concentrated to 12 mg/mL and initial crystallization screening was carried out by the sitting-drop vapor-diffusion method using centrifugal concentrators (Millipore, 10 KDa cutoff). 1 μL protein solution and 1 μL reservoir solution were mixed in a 1:1 ratio and initial screening of crystallization conditions was carried out by JCSG-Plus MD1-37 conditions. Flake-like crystal appeared after 3–4 days from condition No.49 and coincide the diffraction quality.

2.3. Data collection and processing

The crystals were transferred to a cryoprotectant consisting of the crystallization reagent plus 25% (V/V) glycerol (Supplementary Table 2). Then, the crystals were picked up in a nylon loop and then quickly put in at 100 K in canister which full of liquid nitrogen. X-ray diffraction data were collected from a single crystal on beamline BL17U1, a total of 180 frames were recorded with a 1 oscillation angle and 0.2 S exposure time. The data were indexed, integrated and scaled with the HKL3000 program package. Details of the data-processing statistics are provided in (Supplementary Table 3).

2.4. Structure solution and refinement

The structure of ClA1 was determined and refined using the phenix suite program. Initial phase was determined using phaser with the structure of SalL (PDB entry 6RZ2) as a search model [29]. Model building was performed using Coot [30]. The resulting model was refined with phenix.refine [31]. Ramachandran plot of 271 residues and the quality of the structure were evaluated with MolProbity [32]. The final model was deposited in the Protein Data Bank with accession code 7CCG. *PyMOL* was used to present the structure. Refinement statistics are summarized in Supplementary Table 4.

3. Result and discussion

3.1. Determination of the structure of ClA1

The His6-tag-fused recombinant ClA1 protein was expressed in *E. coli*. After adding protein inhibitor, the purified ClA1 was analyzed by SDA-PAGE which showed molecular mass of 28 KDa. The value agrees well with the calculated value of 28.26 KDa for ClA1. The plate-like crystals were grown in sitting drops at 289.15 K within a week and the largest crystal grew to dimensions of approximately 0.7 × 0.4 × 0.06 mm. A complete data set was collected to 1.85 Å resolution.

3.2. Structure description

To understand the structural basis for the catalysis mechanism of ClA1, we determined the high-resolution crystal structure of ClA1. ClA1 have 271 residues and contains large N-terminal domain (residues at 1–151), a linker region (residues at 152–179) and a small C-terminal domain (residues at 180–271). ClA1 shares 59.65% sequence identity with SalL from *Salinispora tropica* [5]. Multiple sequence alignments show the conserved residues located at the enzyme activity site of different chlorinases (ClA1, ClA2 and SalL) and fluorinase (FlA) from *Streptomyces cattleya*, like Asp11, Tyr70, Trp129, Gly131, Asp183, Asn188, Tyr239, Arg243, Leu250 and Gln252 (Fig. 1). Similar with SalL, ClA1 forms oligomers, and the residues in the N-terminal domain of one protomer and the residues in the C-terminal domain of adjacent protomer form the

Fig. 1. Multiple sequence alignment of chlorinases and fluorinases. Sequence alignment was produced by Clustal Omega. The key residues at the binding sits are marked with red asterisks. (For interpretation of the references to colour in this figure legend, the reader is referred to the Web version of this article.)

enzyme activity site. The N-terminal of ClA1 structure is very similar to that of SalL, but their C-terminal structures are more different. The (|Fo |−|Fc|) map for the reaction product shows that 5′-ClDA fits perfect with electron-density. 5′-ClDA shares conserved hydrogen bonds with active sites includes the residues Asp11, Gly131, Asn189, Leu249 and Gln251. 5′-ClDA is well sequestered and buried in the ClA1. The second product is L-methionine which interacted with C-terminal residues of ClA1 and forms hydrogen bonds with Asp184 and Ser241. Compared with 5′-ClDA, L-methionine is more flexible. The side chain conformation of Arg242 in ClA1 is more closed to L-methionine (Fig. 2A).

3.3. The substrate-binding

ClA1, ClA2, SalL and FlA have higher sequence similarity in the N-terminal domain. The difference is centered on the C-terminal domain. The important residues located in the active sites of SalL and ClA1 are almost the same, but the sequence in the active sites of ClA2 is a little different from that in SalL. Moreover, the sequences in the active sites have more differences between FlA and ClA1. We analyzed the structure of ClA1, and the conformational change of Arg242 can be observed obviously (Fig. 2B). Sun et al. measured the kinetic values of SalL and ClA1 for the chlorination reactions [10], and the result shows that the two chlorinases have different catalytic efficiencies. Interestingly, ClA1 appears a more efficient chlorinase than SalL. The K_{cat} value of ClA1 (6.94 ± 0.34 min^{-1}) is higher than the K_{cat} value of SalL (0.89 ± 0.01min^{-1}). And the K_{cat}/K_m value of ClA1 (0.46 $mM^{-1}min^{-1}$) is also higher than that of SalL (0.4 $mM^{-1}min^{-1}$).

We determined the high-resolution crystal structure of ClA1. The conformation of 5′-ClDA is fixed, as 5′-ClDA interacts with surrounding residues to form several hydrogen bonds, like Asp11, Gly131, Asn189, Leu249 and Gln251. Notably, the side chain conformation of Arg242 in ClA1 is obviously different from Arg243 in SalL in complex with 5′-ClDA (PDB: 2Q6I) which is further away from L-Met than Arg242's (Fig. 2C), but that is similar to that in SalL which is complex with SAM (PDB: 6RYZ) (Fig. 2D). Based on the electron density map, L-methionine is observed to be in a dynamic state held in the active site of ClA1. The movement of L-methionine may lead to the conformation alteration of Arg242 into a closer interaction with L-methionine. We also obtained another ClA1 crystal structure with a lower resolution and no products are located at the enzyme activity site. Thus, we supposed that the current structure of ClA1 is probably one of the transient states in the chlorinate reaction. Furthermore, Arg242 facing closely toward L-methionine can stabilize the products formed by the chlorinate reaction. The difference of the side chain conformation of Arg242 could possibly explain the difference of catalytic efficiency between ClA1 and SalL. In future, we plan to further probe the structure-function relationship through more designs of mutagenesis and kinetic assays.

Halogenated metabolites have been proved to have effective medical value. The crystal structure of ClA1 provides the mechanistic details, like the enzyme active sites and is helpful to develop

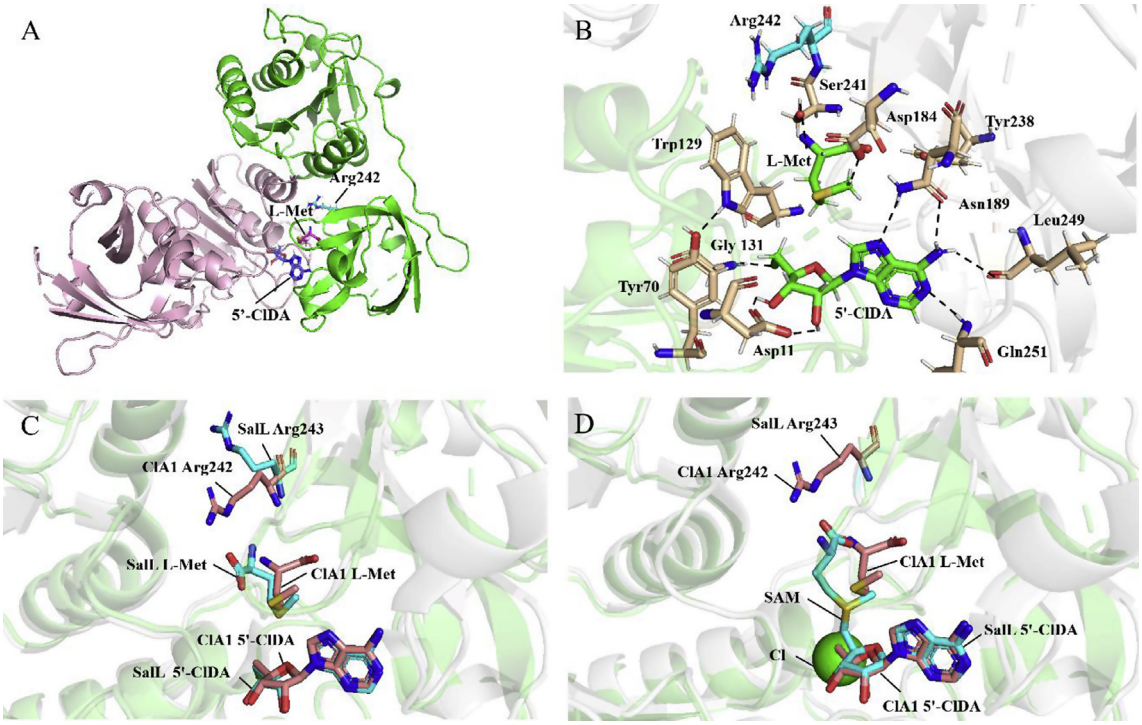

Fig. 2. Crystal structure of ClA1. (A)The overall structure of the ClA1. (cartoon; chain A, light red; chain B, green; 5′-ClDA, purple; L-Met, fuchsia; Arg242, cyan). (B) Close-up view of the active site of ClA1 with bound products 5′-ClDA and L-Met. (The active sites of amino acid residue, gold; 5′-ClDA and L-Met, green; Hydrogen bond, dashed line). (C) Wild-type SalL in complex with 5′-ClDA and L-Met (PDB 2Q6I) superimposed with ClA1 (PDB 7CCG) (Neighbouring monomers of SalL, gray; ClA1, green; Arg243, L-Met and 5′-ClDA of SalL and Arg242, L-Met and 5′-ClDA are shown in cyan and pink respectively). (D) Wild-type SalL in complex with substrates Cl^- and SAM (PDB 6RZ2) superimposed with ClA1 (PDB 7CCG) (SalL, gray; ClA1, green; Arg243, L-Met and 5′-ClDA of SalL, cyan; Arg242, L-Met and 5′-ClDA, pink; Cl^-, dark green). The figures were made using *PyMol*. (For interpretation of the references to colour in this figure legend, the reader is referred to the Web version of this article.)

new biomimetic halogenation catalysts or related enzymes. It is worth noting that analyzing the structure also tell us evolution of the enzyme. SalL is from some bacteria in the marine water, but ClA1 is from soil bacteria. Interestingly, the two chlorinases have very similar activity sites except the sidechain conformation of the conserved arginine. The structure information may be helpful for designing more active chlorinase.

Declaration of competing interest

The authors declare that they have no known competing financial interests or personal relationships that could have appeared to influence the work reported in this paper.

Acknowledgements

This work was supported by the Undergraduate Training Programs for Innovation and Entrepreneurship (HUST: SK2020060). We acknowledge the staff at the BL17U1 beam line of Shanghai Synchrotron Radiation Facility (SSRF) for data collection and processing.

Appendix A. Supplementary data

Supplementary data related to this article can be found at https://doi.org/10.1016/j.bbrc.2020.06.129.

References

[1] T.D. Davis, S. Kunakom, M.D. Burkart, A.S. Eustaquio, Methods Enzymol. 604 (2018) 367–388.
[2] M. Thomsen, S.B. Vogensen, J. Buchardt, M.D. Burkart, R.P. Clausen, Org. Biomol. Chem. 11 (2013) 7606–7610.
[3] M. Ohashi, F. Liu, Y. Hai, M. Chen, M.C. Tang, Z. Yang, M. Sato, K. Watanabe, K.N. Houk, Y. Tang, Nature 549 (2017) 502–506.
[4] C. Dong, F. Huang, H. Deng, C. Schaffrath, J.B. Spencer, D. O'Hagan, J.H. Naismith, Nature 427 (2004) 561–565.
[5] A.S. Eustaquio, F. Pojer, J.P. Noel, B.S. Moore, Nat. Chem. Biol. 4 (2008) 69–74.
[6] V. Agarwal, Z.D. Miles, J.M. Winter, A.S. Eustaquio, A.A. El Gamal, B.S. Moore, Chem. Rev. 117 (2017) 5619–5674.
[7] C. Dalhoff, G. Lukinavičius, S. Klimašauskas, E. Weinhold, Nat. Protoc. 1 (2006) 1879–1886.
[8] A.K. Sinhababu, R.L. Bartel, N. Pochopin, R.T. Borchardt, J. Am. Chem. Soc. 107 (1985) 7628–7632.
[9] J.M. Lipson, M. Thomsen, B.S. Moore, R.P. Clausen, J.J. La Clair, M.D. Burkart, Chembiochem 14 (2013) 950–953.
[10] H. Sun, H. Zhao, E.L. Ang, Chem. Commun. 54 (2018) 9458–9461.
[11] L.C. Blasiak, C.L. Drennan, Acc. Chem. Res. 42 (2009) 147–155.
[12] K.H. van Pee, Methods Enzymol. 516 (2012) 237–257.
[13] D.G. Fujimori, C.T. Walsh, Curr. Opin. Chem. Biol. 11 (2007) 553–560.
[14] D. O'Hagan, D.B. Harper, J. Fluor. Chem. 100 (1999) 127–133.
[15] V.M. Dembitsky, Nat. Prod. Commun. 1 (2006) 127–139.
[16] B.E. Jugder, H. Ertan, M. Lee, M. Manefield, C.P. Marquis, Trends Biotechnol. 33 (2015) 595–610.
[17] A.J. Kale, R.P. McGlinchey, A. Lechner, B.S. Moore, ACS Chem. Biol. 6 (2011) 1257–1264.
[18] T. Kurihara, N. Esaki, Chem. Rec. 8 (2008) 67–74.
[19] F.H. Vaillancourt, E. Yeh, D.A. Vosburg, S. Garneau-Tsodikova, C.T. Walsh, Chem. Rev. 106 (2006) 3364–3378.
[20] C.S. Neumann, D.G. Fujimori, C.T. Walsh, Chem. Biol. 15 (2008) 99–109.
[21] Harris, C. M., Kannan, R., Kopecka, H. & Harris, T. M. (1986). **17**.
[22] R.H. Feling, G.O. Buchanan, T.J. Mincer, C.A. Kauffman, P.R. Jensen, W. Fenical, Angew Chem. Int. Ed. Engl. 42 (2003) 355–357.
[23] L.A. Maldonado, W. Fenical, P.R. Jensen, C.A. Kauffman, T.J. Mincer, A.C. Ward, A.T. Bull, M. Goodfellow, Int. J. Syst. Evol. Microbiol. 55 (2005) 1759–1766.
[24] P.G. Williams, G.O. Buchanan, R.H. Feling, C.A. Kauffman, P.R. Jensen, W. Fenical, J. Org. Chem. 70 (2005) 6196–6203.
[25] Voorhees, P. M., Dees, E. C., O'Neil, B. & Orlowski, R. Z. (2003). 9, 6316-6325.
[26] D. Chauhan, L. Catley, G. Li, K. Podar, T. Hideshima, M. Velankar, C. Mitsiades, N. Mitsiades, H. Yasui, A. Letai, H. Ovaa, C. Berkers, B. Nicholson, T.-H. Chao, S.T.C. Neuteboom, P. Richardson, M.A. Palladino, K.C. Anderson, Canc. Cell 8 (2005) 407–419.
[27] M. Groll, R. Huber, B.C. Potts, J. Am. Chem. Soc. 128 (2006) 5136–5141.

[28] E. Araújo, A.H. Lima, J. Lameira, Phys. Chem. Chem. Phys. 19 (2017) 21350–21356.
[29] I.J.W. McKean, J.C. Sadler, A. Cuetos, A. Frese, L.D. Humphreys, G. Grogan, P.A. Hoskisson, G.A. Burley, Angew Chem. Int. Ed. Engl. 58 (2019) 17583–17588.
[30] P. Emsley, B. Lohkamp, W.G. Scott, K. Cowtan, Acta Crystallogr. D Biol. Crystallogr. 66 (2010) 486–501.
[31] P.V. Afonine, R.W. Grosse-Kunstleve, N. Echols, J.J. Headd, N.W. Moriarty, M. Mustyakimov, T.C. Terwilliger, A. Urzhumtsev, P.H. Zwart, P.D. Adams, Acta Crystallogr. D Biol. Crystallogr. 68 (2012) 352–367.
[32] V.B. Chen, W.B. Arendall 3rd, J.J. Headd, D.A. Keedy, R.M. Immormino, G.J. Kapral, L.W. Murray, J.S. Richardson, D.C. Richardson, Acta Crystallogr. D Biol. Crystallogr. 66 (2010) 12–21.